Comparative Study for Selective Lithium Recovery via Chemical Transformations during Incineration and Dynamic Pyrolysis of EV Li-Ion Batteries

Srija Balachandran [1], Kerstin Forsberg [1], Tom Lemaître [2], Nathália Vieceli [2], Gabriele Lombardo [2] and Martina Petranikova [2,*]

[1] Department of Chemical Engineering, KTH Royal Institute of Technology, School of Engineering Sciences in Chemistry, Biotechnology and Health, 10044 Stockholm, Sweden; srija@kth.se (S.B.); kerstino@kth.se (K.F.)

[2] Department of Chemistry and Chemical Engineering, Industrial Materials Recycling and Nuclear Chemistry, Chalmers University of Technology, 41296 Gothenburg, Sweden; tom.lemaitre14@gmail.com (T.L.); nathalia.vieceli@chalmers.se (N.V.); lombardgabriele@gmail.com (G.L.)

* Correspondence: martina.petranikova@chalmers.se

Abstract: Selective leaching of Li from spent LIBs thermally pretreated by pyrolysis and incineration between 400 and 700 °C for 30, 60, and 90 min followed by water leaching at high temperature and high L/S ratio was examined. During the thermal pretreatment Li_2CO_3 and LiF were leached. Along with Li salts, AlF_3 was also found to be leached with an efficiency not higher than 3.5%. The time of thermal pretreatment did not have a significant effect on Li leaching efficiency. The leaching efficiency of Li was higher with a higher L/S ratio. At a higher leaching temperature (80 °C), the leaching of Li was higher due to an increase in the solubility of present Li salts. The highest Li leaching efficiency of nearly 60% was observed from the sample pyrolyzed at 700 °C for 60 min under the leaching condition L/S ratio of 20:1 mL g^{-1} at 80 °C for 3 h. Furthermore, the use of an excess of 10% of carbon in a form of graphite during the thermal treatment did not improve the leaching efficiency of Li.

Keywords: electric vehicles; Li-ion batteries; a combined method of recycling; pyrolysis; incineration; water leaching

1. Introduction

The average life span of Li-ion batteries (LIBs) in electric vehicles (EVs) is expected to be around 8–10 years. This will result in the generation of a huge number of spent LIBs somewhere between 1.1 million tons by 2030 to 5.3 million tons by 2040 in the EU [1]. The disposal of these batteries not only has several environmental impacts due to toxic and flammable electrolytes and other hazards but also results in the loss of valuable metals as waste. Therefore, efficient, and sustainable recycling methods should also grow at the same pace as the EV industries; otherwise, there will be a rapid depletion of metals from the primary supplies. Particularly, recycling cathode materials will have a huge effect from an environmental standpoint, contribute to reducing battery cost and ensure a sustainable supply of materials in the long run [2,3].

Lithium is one of the vital elements for the modern energy revolution and there is an increasing demand for its usage in battery applications. For example, it is projected that the demand for Li in LIBs will expand from 9760 tons in 2015 to 21,520 tons in 2025 [4]. Also, there are problems related to the uneven distribution of Li in some geographical locations, which could lead to supply risk. For instance, the main global reserves of Li are mostly concentrated in South America and Australia. It has been predicted that there will be a severe scarcity of Li in the near future [5]. Furthermore, there are high environmental burdens and negative social impacts associated with the extraction of virgin materials [6,7].

Recently, Li was added to the list of the European Union's critical materials due to its high economic importance in battery application and supply risk raised due to dependence on other countries [8,9].

The hydrometallurgical processes are efficient in the recycling of LIBs. However, acid-based leaching processes have some drawbacks related to Li recovery, such as a limited number of extractants available to directly recover Li from the leaching solution. Thus, Li is consequently recovered in the last steps of the hydrometallurgical process. Also, low concentrations of Li are retained in the raffinate at the end of each solvent extraction stage, which makes Li recovery difficult and uneconomical [10]. Acid-based leaching followed by recovery processes involves complex recycling routes and Li loss occurs at numerous points during the recovery of other metals. A significant amount of Li is lost, as Li forms complex salts with sodium, which is used to treat impurities, extract valuable metals and pH adjustment. During these processes, there are huge amounts of organic or mineral acids being consumed. Furthermore, another drawback related to the acid-based leaching process involves the consumption of alkali compounds that are needed to neutralize acid leachate liquor as an alkaline condition (pH ca. 10–12) is suitable for high recovery and purity of Li products [2]. There are problems raised from the generation of large volumes of acid/alkaline waste, sludge containing heavy metal ions, organic waste, negative carbon dust which further create an extra cost for secondary pollution treatment due to the environmental problems [11].

To address the shortcomings related to Li recycling, combined methods to extract Li selectively before extraction of other valuable metals from spent LIBs are found to be a promising route, including for example thermal treatment followed by water leaching. In this context, the aim of this work is to investigate selective leaching of Li from thermally pretreated waste batteries with water as a leaching agent at high temperature and high L/S ratio. The L/S ratio indicates the liquid/solid ratio which is the amount of black mass in 'g' per volume of leaching liquid in 'mL'. Through the combined methods, Li could be recovered first, and other metals will remain in the black mass which could be recovered in later stages and, thus, Li could be more easily separated from other metals. Furthermore, Li salts show good solubility in water and so water is used as a leaching agent.

The removal of organic compounds such as binder (e.g., PVDF—polyvinylidene fluoride), separator, and graphite is promoted by thermal treatment processes. Particularly, the presence of binder hinders the recovery of metals during the hydrometallurgical processes of leaching and solvent extraction. Two main thermal treatment processes are generally applied, namely incineration and pyrolysis, which are the processes taking place in the presence and absence of oxygen, respectively. The carbon acts as a reducing agent, thereby reducing the metal oxides from higher valence states to their lower valence states, which improves the leaching efficiency of some metals during subsequent leaching processes [12]. This is an in-situ recycling process where the electrode material (graphite) is used to facilitate resource recovery together with the carbon from other organic components. This means no additional reagents are needed during this process, which could further minimize the generation of secondary pollution [11]. Thus, the efficiency of material recovery in the hydrometallurgical process could be enhanced by thermal pretreatment [11,13].

Kuzuhara et al. worked on the incineration process for recovery of Li from sample synthesized with LCO ($LiCoO_2$) powder and activated carbon, where a Li recovery of 90% was achieved at 500–600 °C in the form of Li_2CO_3. In addition, to achieve a high Li recovery with high purity, it was suggested to increase the temperature and lower the F/Li ratio in the solution [14]. According to Liu et al. [15], a simple and environmentally friendly method of metal recovery from spent LIBs was proposed, which utilized a combined method of treatment: reduction roasting and hydrometallurgical recovery. The roasting of NMC111 ($LiNi_{1/3}Mn_{1/3}Co_{1/3}O_2$) resulted in products such as Li_2CO_3, Ni, Co, MnO, and NiO, where Li_2CO_3 was first leached with water and the residual solid residue was then subsequently subjected to H_2SO_4 leaching. During this process, a Li leaching efficiency of 93.7% was achieved from the sample roasted at 650 °C for 30 min. In a work performed

by Xiao et al. [11], a combined method to recycle Li as Li_2CO_3 was suggested, where the cathode materials were reduced in-situ with graphite as a reductant under vacuum pyrolysis. Later, Li_2CO_3 was recovered by water leaching. Li recovery rates of 81.9%, 82.7%, and 66.3% were obtained from LMO, LCO, and NMC respectively at 973 K for 30 min with a L/S ratio of 4. Peng et al. [4] carried out an environmentally friendly process by combining oxygen-free roasting and wet magnetic separation, where LCO and graphite were roasted in an oxygen-free atmosphere at 1000 °C for 30 min. The solid residue obtained was then subjected to water leaching where Li was obtained with a high recovery of 98.9% in the form of Li_2CO_3. In a work performed by Jandova et al. [16], a combined process of roasting–leaching–crystallization and condensation–precipitation steps to separate Li_2CO_3 from Li/MnO_2 batteries were applied. Li extraction of about 80% was reached with samples roasted at 650 °C with Li_2CO_3 purity of 99.5% by evaporation of 95% of water. In another work by Paulino et al. [17], two recycling processes were tested. Firstly, the cathode material was treated with a $KHSO_4$ solution and then calcined at 500 °C for 5 h. The thermally treated contents were then leached with distilled water for 1 h at 90 °C. In the next process, incineration of materials was carried out at 500 °C for 5 h and then were leached with water. The result showed an improvement in Li recovery after removing carbon, as carbon could be a strong adsorbent for Li^+ ions. This has resulted in a Li recovery of nearly 90%. From these works, it is evident that hydrometallurgical treatment can be improved by using thermally pretreated battery materials for Li recovery. Even though pyrometallurgical processes have a higher footprint compared to the hydrometallurgical process, a high recovery of Li could be achieved. Thus, thermal pretreatment simplifies hydrometallurgical treatment processes. This work further investigates the comparative study for selective Li recovery from mixed cathode and anode materials of $LiNi_{1/3}Mn_{1/3}Co_{1/3}O_2$ (NMC111) batteries by water leaching exposed to incineration and pyrolysis pretreatments and analyzes the behavior of impurities.

The thermal pretreatment enhances the degradation of cathode materials and results in the formation of water-soluble Li salts. The following section illustrates the mechanism through which Li_2CO_3 was formed during the thermal treatments.

Incineration occurs in the presence of oxygen. The high temperature results in the combustion of graphite and organic compounds and the formation of CO_2 and CO according to Equations (1)–(3) [12]. In the presence of O_2, $LiCoO_2$ is reduced by C and CO to Co_3O_4, Li_2CO_3, and CO_2 according to Equations (4) and (5), $LiMn_2O_4$ is reduced by C and CO to Mn_3O_4, MnO_2, Li_2O, and CO_2 according to Equations (6)–(9). Furthermore, Li_2O reacts with $CO_{2(g)}$ to form Li_2CO_3 according to Equations (10) and (11). Similarly, in the presence of O_2, $LiNiO_2$ is reduced by C and CO to Ni_3O_4, Li_2CO_3, and CO_2 according to Equation (12).

$$C_{(s)} + O_{2(g)} \rightarrow CO_{2(g)} \tag{1}$$

$$2\,C_{(s)} + O_{2(g)} \rightarrow 2\,CO_{(g)} \tag{2}$$

$$2\,CO_{(g)} + O_{2(g)} \rightarrow 2\,CO_{2(g)} \tag{3}$$

$$3\,LiCoO_{2(s)} + 2.5\,C_{(s)} + 2.25\,O_{2(g)} \rightarrow Co_3O_4 + 1.5\,Li_2CO_{3(s)} + CO_{2(g)} \tag{4}$$

$$3\,LiCoO_{2(s)} + 2.5\,CO_{(g)} + O_{2(g)} \rightarrow Co_3O_4 + 1.5\,Li_2CO_{3(s)} + CO_{2(g)} \tag{5}$$

$$12\,LiMn_2O_{4(s)} + 6\,C_{(s)} + O_{2(g)} \rightarrow 8\,Mn_3O_{4(s)} + 6\,Li_2O_{(s)} + 6\,CO_{2(g)} \tag{6}$$

$$6\,LiMn_2O_{4(s)} + 5\,CO_{(g)} \rightarrow 4\,Mn_3O_{4(s)} + 3\,Li_2O_{(s)} + 5\,CO_{2(g)} \tag{7}$$

$$2\,LiMn_2O_{4(s)} + C_{(s)} + 1.5\,O_{2(g)} \rightarrow 4\,MnO_{2(s)} + Li_2O_{(s)} + CO_{2(g)} \tag{8}$$

$$2\,LiMn_2O_{4(s)} + CO_{(g)} + O_{2(g)} \rightarrow 4\,MnO_{2(s)} + Li_2O_{(s)} + CO_{2(g)} \tag{9}$$

$$Li_2O_{(s)} + CO_{2(g)} \rightarrow Li_2CO_{3(s)} \tag{10}$$

$$2\,Li_2O_{(s)} + 2\,CO_{(g)} + O_{2(g)} \rightarrow 2\,Li_2CO_{3(s)} \tag{11}$$

$$3\,LiNiO_2 + 2.5\,C_{(s)} + 2.25\,O_{2(g)} \rightarrow Ni_3O_4 + 1.5\,Li_2CO_{3(s)} + CO_{2(g)} \tag{12}$$

The pyrolysis process takes place in a nitrogen atmosphere. The carbothermic reduction of metal oxides is favored by the carbon present in the sample through a CO intermediate, along with the formation of CO_2 and CO [16]. $LiCoO_2$ is converted to Co, CoO, Li_2O, CO, and CO_2 at high temperatures according to Equations (13)–(17). Thus, Li_2O formed results in the formation of Li_2CO_3 reacting with CO_2 (Equation (10)). Also, $LiCoO_2$ is converted to Co, Li_2CO_3, and gases (CO and CO_2) according to Equations (18) and (19). Thus, the main products of carbothermic reduction are Co and Li_2CO_3. $LiMn_2O_4$ is converted to Mn_3O_4, Li_2CO_3, Li_2O, MnO, CO, and CO_2, according to Equations (20)–(22). $LiNiO_2$ is converted to Ni, Li_2CO_3, Li_2O, NiO, CO, and CO_2 according to Equations (23)–(27).

$$4\,LiCoO_{2(s)} + 3\,C_{(s)} \rightarrow 2\,Li_2O_{(s)} + 4\,Co_{(s)} + 3\,CO_{2(g)} \tag{13}$$

$$4\,LiCoO_{2(s)} + C_{(s)} \rightarrow 2\,Li_2O_{(s)} + 4\,CoO_{(s)} + CO_{2(g)} \tag{14}$$

$$2\,LiCoO_{2(s)} + 3\,C_{(s)} \rightarrow Li_2O_{(s)} + 2\,Co_{(s)} + 3\,CO_{(g)} \tag{15}$$

$$2\,LiCoO_{2(s)} + C_{(s)} \rightarrow Li_2O_{(s)} + 2\,CoO_{(s)} + CO_{(g)} \tag{16}$$

$$2\,LiCoO_{2(s)} + 3\,CO_{(g)} \rightarrow Li_2O_{(s)} + 2\,Co_{(s)} + 3\,CO_{2(g)} \tag{17}$$

$$2\,LiCoO_{2(s)} + 3\,CO_{(g)} \rightarrow 2\,Co_{(s)} + Li_2CO_{3(s)} + 2\,CO_{2(g)} \tag{18}$$

$$6\,LiCoO_{2(s)} + 5\,C_{(s)} \rightarrow 6\,Co_{(s)} + 3\,Li_2CO_{3(s)} + CO_{2(g)} + CO_{(g)} \tag{19}$$

$$2.4\,LiMn_2O_{4(s)} + C_{(s)} \rightarrow 1.2\,Li_2O_{(s)} + 1.6\,Mn_3O_{4(s)} + CO_{2(g)} \tag{20}$$

$$3\,LiMn_2O_{4(s)} + 2.5\,CO_{(g)} \rightarrow 2\,Mn_3O_{4(s)} + 1.5\,Li_2CO_{3(s)} + CO_{2(g)} \tag{21}$$

$$2\,LiMn_2O_{4(s)} + 2\,C_{(s)} \rightarrow Li_2CO_{3(s)} + 4\,MnO_{(s)} + CO_{(g)} \tag{22}$$

$$4\,LiNiO_{2(s)} + C_{(s)} \rightarrow 2\,Li_2O_{(s)} + 4\,NiO_{(s)} + CO_{2(g)} \tag{23}$$

$$2\,LiNiO_{2(s)} + 3\,C_{(s)} \rightarrow Li_2O_{(s)} + 2\,Ni_{(s)} + 3\,CO_{(g)} \tag{24}$$

$$2\,LiNiO_{2(s)} + C_{(s)} \rightarrow Li_2O_{(s)} + 2\,NiO_{(s)} + CO_{(g)} \tag{25}$$

$$2\,LiNiO_2(s) + 3\,CO_{(g)} \rightarrow 2\,Ni_{(s)} + Li_2CO_{3(s)} + 2\,CO_{2(g)} \tag{26}$$

$$6\,LiNiO_{2(s)} + 5\,C_{(s)} \rightarrow 6\,Ni_{(s)} + 3\,Li_2CO_{3(s)} + CO_{2(g)} + CO_{(g)} \tag{27}$$

2. Materials and Methods

2.1. Thermal Treatment

The NMC111 type batteries used for this work were provided by Volvo Cars (Sweden). The batteries were first dismantled to remove the plastic cover and then both electrodes (cathode and anode) and the separator were cut into small pieces manually. The samples were then subjected to two different thermal treatment processes in the temperature range between 400 and 700 °C under different treatment times (30, 60, and 90 min), as described by Lombardo et al. [12]. For all of the experiments, equal quantities of mixed electrodes along with the separator were used, except for the test performed with excess graphite, where 10% more graphite was added.

2.2. Chemicals Used

For the experiments, Nitric acid (HNO_3, ≥69%, ACS reagent, Sigma-Aldrich, St. Louis, MO, USA), hydrochloric acid (HCl, 37%, ACS reagent, Sigma-Aldrich, St. Louis, MO, USA), Milli-Q water, and a syringe filter (0.45 µm, Fischer Scientific, Hampton, NH, USA) were used.

2.3. Analytical Techniques

The total concentration of metals in the samples after thermal treatment was determined by ICP–OES (Inductively Coupled Plasma—Optical Emission Spectrometry) using an iCAP™ 6000 Series ICP-OES (Thermo Fisher Scientific, Waltham, MA, USA). Aqua regia (HCl: HNO_3 = 3:1) was used to digest the thermally pretreated samples using a hot plate at approximately 80 °C and magnetic stirring for 5 h. After digestion, the samples were filtered using a syringe filter and diluted using 0.5 M HNO_3 solution to determine their elemental composition by ICP-OES analysis.

X-ray powder diffraction (XRPD) was used to characterized the solid samples and it was conducted using a Siemens D5000 X-ray diffractometer, Midland, ON, Canada with an accelerator voltage of 40 kV and a current of 40 mA. Cu K-radiation was used, and the scans included a 2Θ range from 10° to 100°. Also, a sample rotation speed of 15 rpm was set. The diffraction data obtained were identified by comparing with standard data for known compounds using JCPDS database.

2.4. Leaching Experiment and Analytical Procedure

Leaching experiments were carried out using Milli-Q water as a leaching agent. Both ground untreated and thermally treated samples were used for the experiments. Different L/S ratios (10:1 and 20:1 mL g^{-1}) were used, and the experiments were performed both at room temperature (RT) of around 23 and at 80 °C with a magnetic stirring speed of 300 rpm for 3 h. At the end of each experiment, the leachate was collected and filtered through a syringe filter. Before analyzing the metal content of each sample using ICP-OES, each sample was diluted with 0.5 M HNO_3. By comparing the concentration of each metal in the leachate to the initial metal content in the solid samples obtained by aqua regia digestion, the leaching efficiency was calculated using Equation (28). All of the experiments were performed in triplicate under identical conditions. Using a thermocouple, the solution temperature was measured and the temperature within ±1% set value was maintained by adjusting the heater output.

$$\eta_i = \frac{C_i V}{m_0 \omega i} \times 100 \tag{28}$$

where, C_i (mgL^{-1}) is the concentration of metal ion i in the solution, V (L) is the volume of leaching solution, m_0 (mg) is the mass of pretreated material, and ω_i is the weight content of element i in the sample.

2.5. Evaporative Crystallization

To recover the lithium salts from the leachate, the solution was first filtered using a filter paper to separate the leach residue. The water present in the filtrate was evaporated by heating the solution to 100 °C and the precipitate was collected. Both the leach residue and precipitates were dried (24 h at 80 °C), and different solid phases present in these samples were characterized by XRPD analysis.

3. Results

3.1. Elemental Composition of Solid Samples

The initial weight content of metals determined by the digestion of solid samples in aqua regia obtained at different treatment conditions is tabulated in Table 1. These data were used for the calculation of leaching efficiency.

Table 1. Composition of thermally treated samples and untreated sample.

Treatment	Temperature (°C)	Time (min)	Li (wt.%)	Al (wt.%)
Incineration	Untreated		2.2 ± 0.2	6.2±0.3
	400	30	2.6 ± 0.2	5.9 ± 1.0
		60	2.7 ± 0.1	6.0 ± 0.7
		90	3.3 ± 0.1	9.8 ± 0.2
	500	30	3.2 ± 0.2	11.6 ± 0.3
		60	3.1 ± 0.1	11.4 ± 0.5
		90	2.4 ± 0.2	9.2 ± 0.9
	600	30	2.0 ± 0.0	8.2 ± 0.3
		60	2.8 ± 0.2	10.0 ± 0.2
		90	2.6 ± 0.1	10.3 ± 1.1
	700	30	3.3 ± 0.0	10.1 ± 0.9
		60	3.7 ± 0.0	8.9 ± 0.3
		90	3.6 ± 0.1	9.8 ± 0.3
Pyrolysis	400	30	2.6 ± 0.0	8.5 ± 0.5
		60	2.3 ± 0.1	9.2 ± 0.9
		90	2.6 ± 0.1	9.0 ± 1.1
	500	30	3.0 ± 0.0	8.6 ± 0.3
		60	2.8 ± 1.1	7.8 ± 0.7
		90	2.7 ± 0.0	9.3 ± 0.9
	600	30	2.8 ± 0.0	8.6 ± 0.6
		60	2.9 ± 0.2	8.7 ± 1.1
		90	2.6 ± 0.0	10.3 ± 0.8
	700	30	2.9 ± 0.0	10.3 ± 0.9
		60	3.0 ± 0.1	9.1 ± 0.4
		90	2.5 ± 0.1	10.2 ± 0.7
Pyrolysis with additional carbon	Untreated		3.4 ± 0.7	8.9 ± 0.5
	400	30	3.1 ± 0.1	5.9 ± 0.8
	500	30	3.2 ± 0.0	6.0 ± 0.0
	600	30	3.0 ± 0.4	6.4 ± 0.6
	700	30	3.1 ± 0.2	8.6 ± 1.2

3.2. The Effect of Thermal Treatment on Li Leaching Efficiency

The leaching efficiency of the untreated sample under the leaching condition of L/S ratio of 20:1 mL g^{-1}, 80 °C, and 3 h was found to be only 7.5%. It was possible to recover Li from the lithium salts present in the electrolyte by leaching the untreated sample with water. Figure 1a shows the effect of temperature on the leaching of Li from the products pyrolyzed between 400 and 700 °C. The pyrolysis treatment had a positive effect on the Li leaching efficiency, and it can be seen that the leaching of Li rises with the increase in treatment temperature. At 400 °C, the leaching efficiency was found to be around 10%. The low leaching efficiency could be related to the partial decomposition of metal oxides at the given temperature. The carbothermic reduction of metal oxides was accelerated along with increasing treatment temperatures by C and CO present in the system and resulted in the formation of an increased amount of leachable Li salts, which resulted in an improved leaching efficiency. At 700 °C, 60% of Li was leached, which was the highest among all conditions. The change in thermal treatment time did not have a significant effect on the leaching efficiency of Li, with less than 4% difference, at all the temperatures. This could be because of the unreacted lithium metals oxides that are still present in the samples after 60 min of pyrolysis, which could be seen in the X-ray diffraction analysis (XRD) studies as shown in Figure 2 due to lack of carbothermic reduction agent.

Overall, the leaching efficiency of Li obtained from samples after incineration was much lower than from the pyrolysis which can be seen by comparing Figure 1a,b. This could be because of variation in the kinetics in the oxidation of carbon to CO_2 and the carbothermic reduction of metal oxides. In addition, the leaching efficiency at 400 and

500 °C was similar (nearly 15%) at all the treatment times. However, for 600 and 700 °C, the leaching efficiency was comparatively higher after 30 min and after that, it decreased and reached similar efficiencies as of the other two conditions. At higher temperatures, most of the carbon oxidized to CO_2 before the carbothermic reduction of metal oxides.
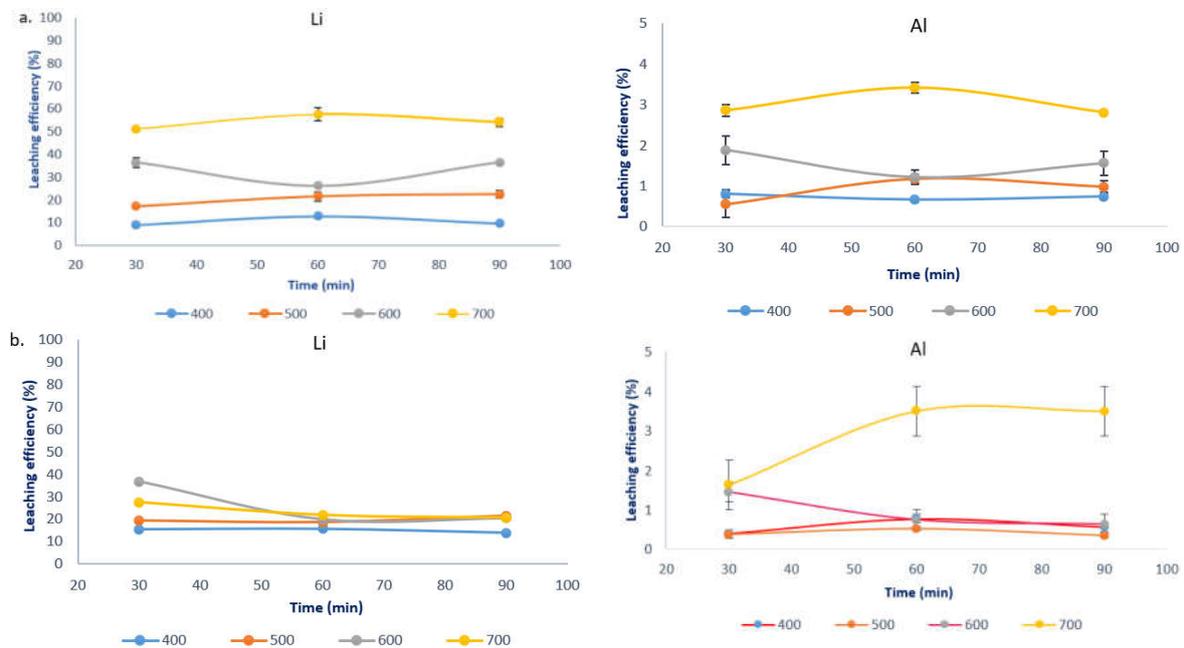

Figure 1. The effect of thermal treatment temperature and time on Li and Al leaching efficiency: (**a**) pyrolysis and (**b**) incineration (Leaching condition: L/S ratio = 20:1 mLg^{-1}, 80 °C, 300 rpm, and 3 h).

3.3. The Effect of L/S Ratio on the Leaching Efficiency of Li

The effect of L/S ratio on the water leaching of Li performed at 80 °C, stirring of 300 rpm for 3 h at two different L/S ratios of 10:1 and 20:1 mL g^{-1}, from samples pyrolyzed and incinerated between 400 and 700 °C for 30, 60, and 90 min are shown in the Figure 3a,b. A similar trend after both pyrolysis and incineration at two different leaching conditions was observed. The leaching efficiency of Li was higher at higher L/S ratio. A larger amount of Li can be dissolved a*t* higher L/S ratio when the dissolution is limited by the solubility. Additionally, the decrease in the pulp density can promote a more efficient mixing effect and facilitate reactions dependent on mass transfer between the solids and the liquid phase.

3.4. The Effect of Leaching Temperature on the Leaching Efficiency of Li

The effect of leaching temperature on the water leaching of Li performed at the stirring of 300 rpm for 3 h with an L/S ratio 20:1 mL g^{-1} at two different leaching temperatures: 80 °C and RT from samples pyrolyzed and calcined between 400 and 700 °C for 30, 60, and 90 min are shown in Figure 4a,b. At a higher leaching temperature, the leaching of Li is higher for all the thermal treatment temperatures. This is due to the increase in solubility of Li salts with the increase in the temperature. Initially, the samples contain Li_2CO_3 which solubility decreases with the increase in the temperature, however, the presence of other Li products and anions (F) that could be more easily leached at higher temperatures could affect the final leaching efficiencies. The formation of LiF by the reaction of Li_2O and Li_2CO_3 with HF generated by the degradation of PVDF binder can happen during the thermal treatment according to Equations (29) and (30) [18,19]. The presence of LiF was also confirmed by XRD analysis of the samples by using the powder (from pyrolysis 30 min at 700 °C) obtained after the evaporative crystallization of the leaching solution free of

leaching residue as shown in Figure 5. Therefore, due to the presence of a mixture of Li salts, the decrease in solubility of Li_2CO_3 with an increase in temperature might deviate.

$$Li_2O + 2\ HF \rightarrow 2\ LiF + H_2O \tag{29}$$

$$Li_2CO_3 + 2\ HF \rightarrow 2\ LiF + H_2O + CO_2 \tag{30}$$
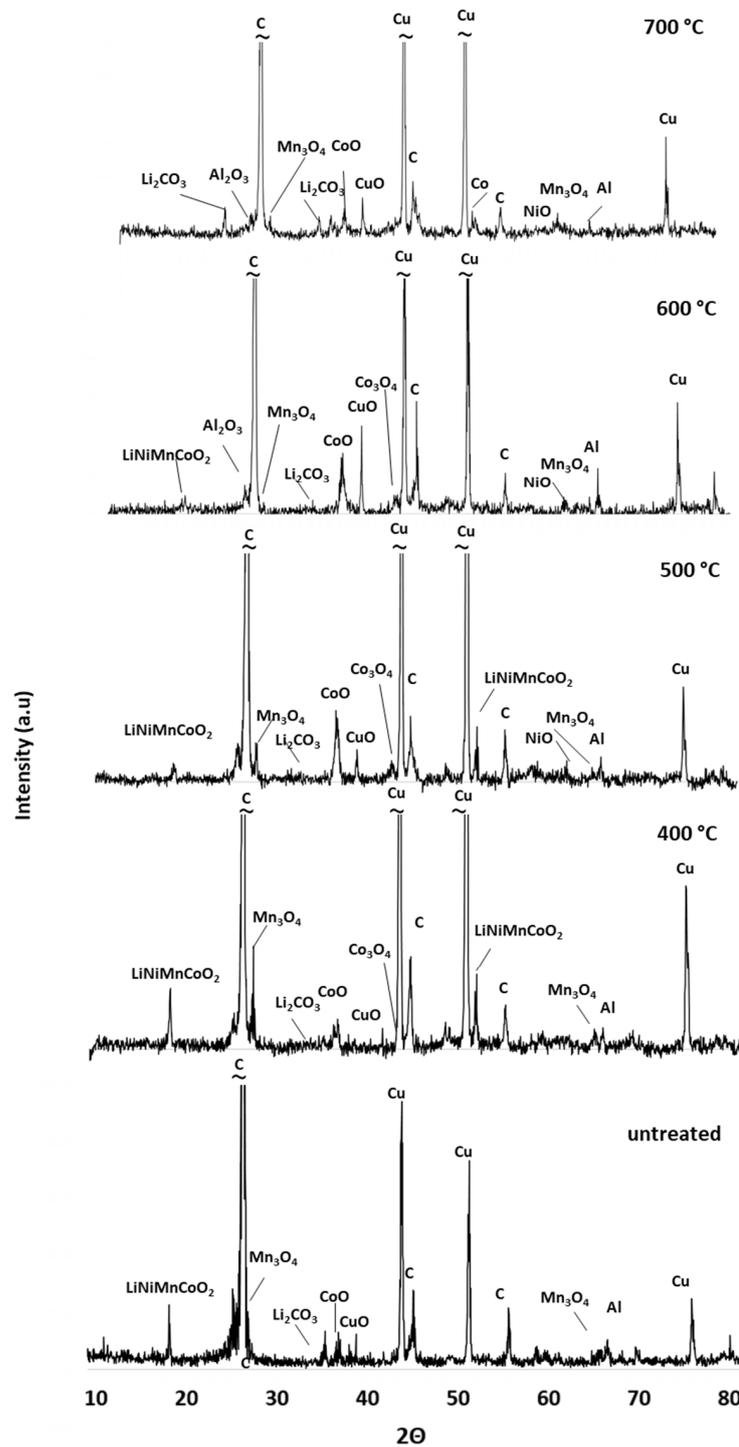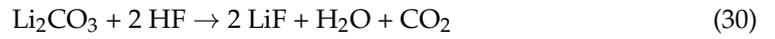
Figure 2. XRD diffractograms of samples after 60 min of pyrolysis at 400, 500, 600, and 700 °C.
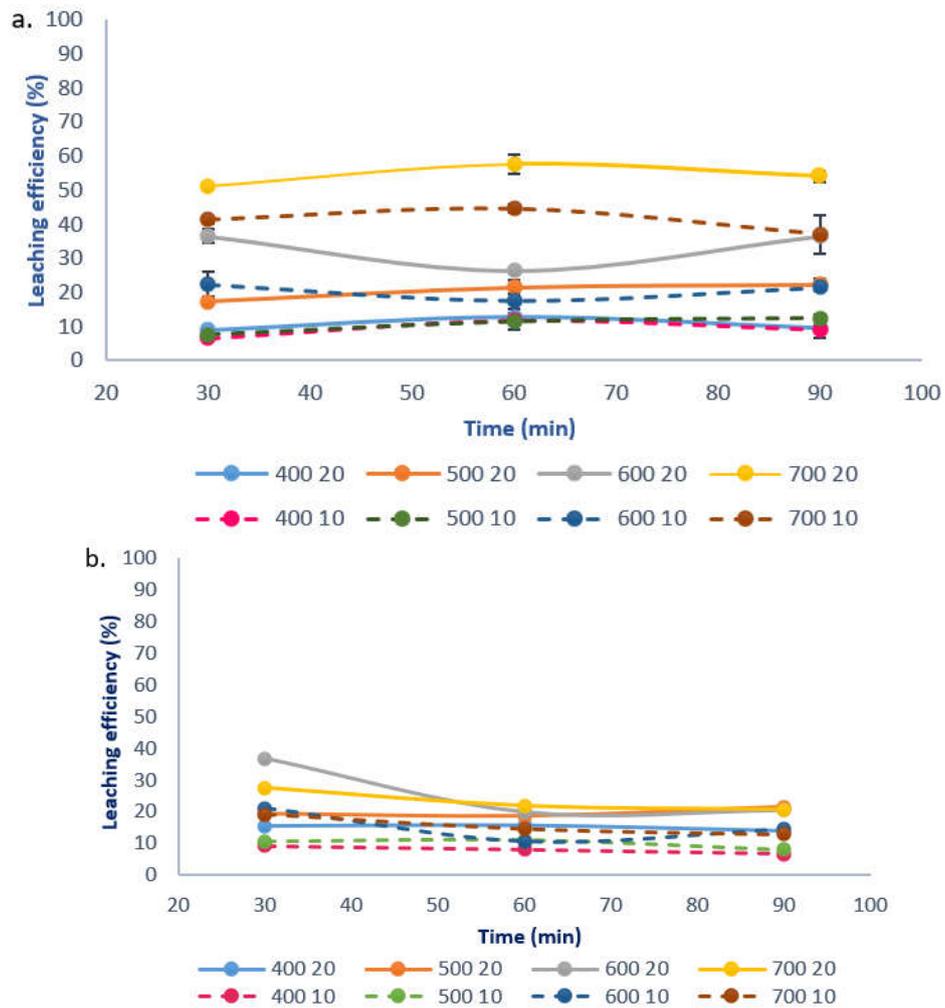
Figure 3. The effect of L/S ratio on Li leaching efficiency: (**a**) pyrolysis and (**b**) incineration (Leaching condition: L/S ratio = 20:1 and 10:1 mL g^{-1}, 80 °C, 300 rpm, and 3 h).
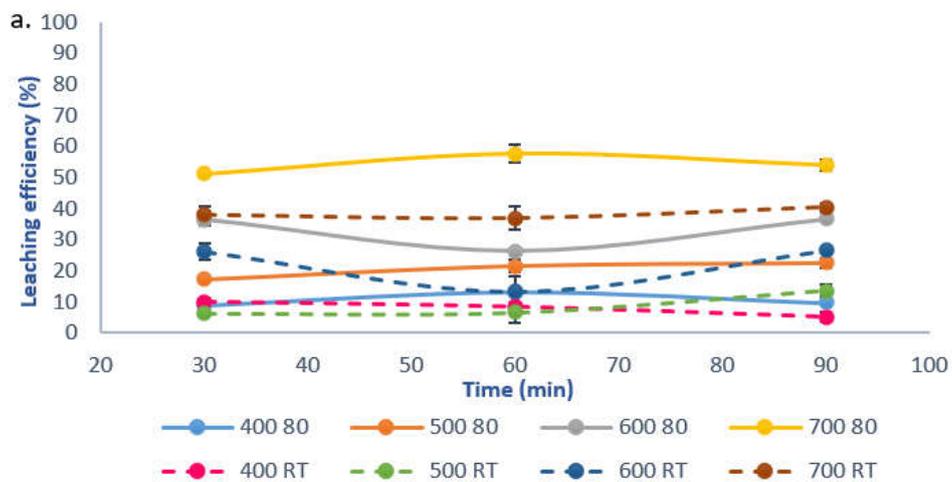

Figure 4. *Cont.*
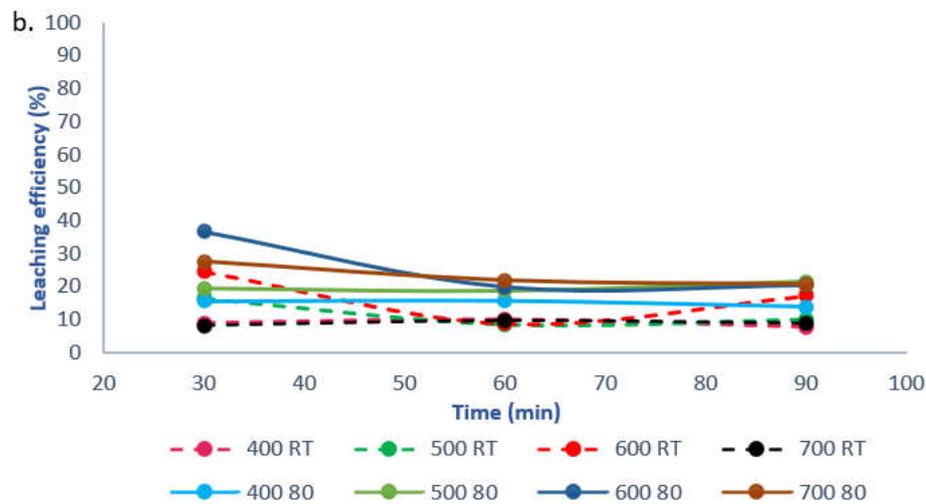
Figure 4. The effect of leaching temperature on Li leaching efficiency: (**a**) pyrolysis and (**b**) incineration (Leaching condition: (**a**). L/S ratio = 20:1 mL g^{-1}, 80 °C and RT, 300 rpm, and 3 h). RT: room temperature.
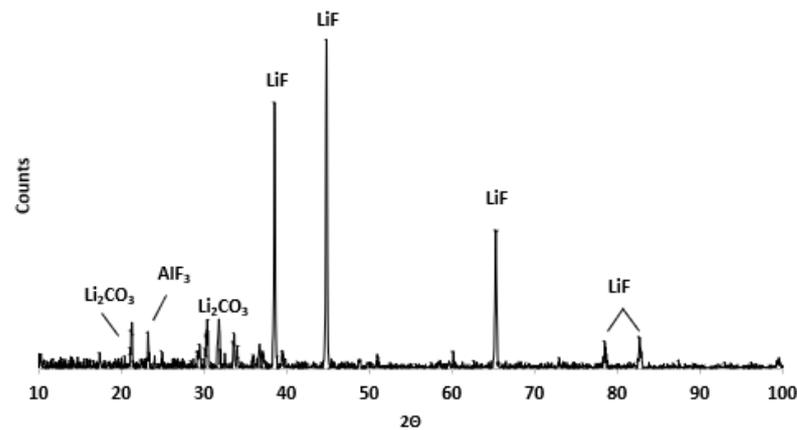

Figure 5. XRD diffractogram of crystallization product of the solution after leaching pyrolyzed sample (700 °C and 30 min).

The results from XRD studies carried out using leaching residues from pyrolysis treatment at different temperatures and leached with water using an L/S ratio of 20:1 mL g^{-1}, 80 °C, and 300 rpm for 3 h are shown in Figure 6. Also, the result from thermally untreated samples is shown. The untreated sample predominantly shows the presence of NMC cathode materials and graphite (represented in the diffractograms as C) and there is no formation of leachable Li salts. After the thermal pretreatment, the intensity of the peaks of NMC oxides decreased when compared to the untreated sample which could be explained by the reduction of the mixed oxides during the thermal treatment. Yet, there are some unreacted NMC materials still present after the thermal pretreatment which indicates that not all NMC materials were reduced. In addition, at 600 and 700 °C, peaks of Li_2CO_3 and LiF were seen in the leaching residue which indicated that Li salts were not completely leached. Therefore, the reasons for the low efficiency (only nearly 60%, which was the maximum efficiency achieved among all the experimental results) of Li could be either due to the presence of unreacted NMC cathode materials in the sample or not all Li salts formed were completely leached with water (e.g., oxide, Li_2O).

3.5. Effect of Addition of Excess Carbon

The XRD analysis results at different thermal treatment conditions shown in Figure 6 show the presence of peaks of NMC cathode materials which means that some Li is

being trapped in the unconverted cathode possibly due to the lack of available carbon for reduction. So, an excess of carbon was added to test if an excessive amount of carbon would be beneficial to promote a more complete carbothermic reduction of NMC material. The effect of using excess carbon on leaching of Li performed at the stirring of 300 rpm for 1 h with an L/S ratio 20:1 mL g^{-1} at 80 °C from samples pyrolyzed at 400, 500, 600, and 700 °C for 30 min is shown in Figure 7. It can be observed that not much improvement in leaching of Li was observed by having additional carbon during the thermal pretreatment and the maximum efficiency was found to be nearly 30%. This could be because graphite being a stable form of carbon and does not help in enhancing leaching efficiency. A decrease in the leaching efficiency was observed which might be due to the presence of carbon which could act as an adsorbent for Li$^+$ ions and further decrease the leaching efficiency, as stated in [17]. Therefore, the addition of excess graphite did not have a significant effect on the leaching of Li.

Another method to improve Li leachability can be with the use of supercritical CO_2 as reported in [20], where Li efficiency was 79%.
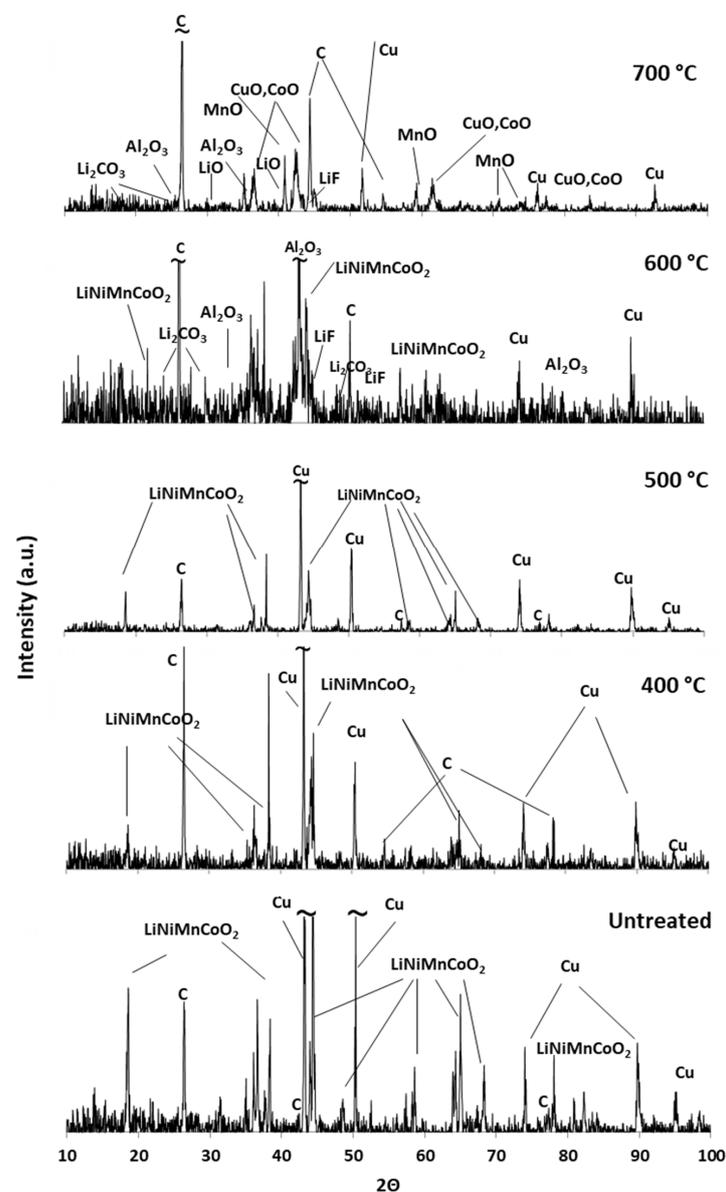

Figure 6. XRD diffractogram of residue after leaching pyrolyzed samples.
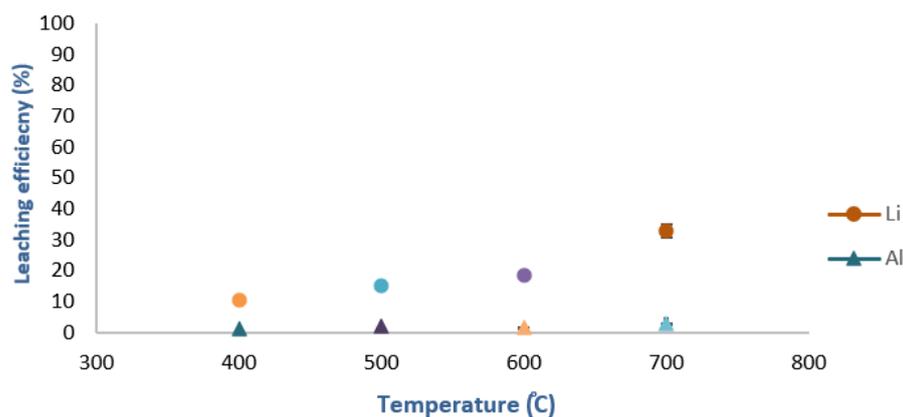
Figure 7. The effect of 10% excess of carbon on leaching of Li and Al from pyrolyzed samples. (Leaching condition: L/S ratio = 20:1 mL g^{-1}, 80 °C, 300 rpm, and 1 h).

3.6. Leaching of Al

Al exits in both untreated and thermally treated samples in different forms such as alloys, metallic Al, salts, and Al_2O_3 which could be formed by the oxidation of Al. However, the presence of salts was not detected by XRD analysis. Along with Li, a very small amount of Al was also found to be leached at all the treatment conditions. Al was found in the form of AlF_3 in the leaching residue of the thermally pretreated samples. This may be from the AlF_3 used as a protective coating for the electrode materials [21,22] or could be formed by the reaction of HF with Al and Al_2O_3 according to Equations (31) and (32) [23,24]. Also, the presence of AlF_3 was confirmed in the XRD analysis of the crystallization product as shown in Figure 4. Although Al_2O_3 was observed in XRD analysis, it is not expected to be leached with water as it shows resistance to acid attack, even by aqua regia [12]. However, the Al leaching efficiency in the sample obtained from both thermal treatments was not higher than 3.5%.

$$2. \; Al + 6\,HF \rightarrow 2\,AlF_3 + 3\,H_2 \tag{31}$$

$$Al_2O_3 + 6\,HF \rightarrow 2\,AlF_3 + 3\,H_2 \tag{32}$$
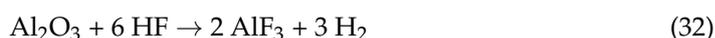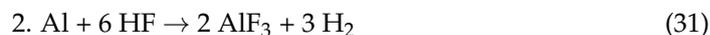
3.7. Effect of Thermal Treatment Temperature on the Leaching Efficiency of Al

The effect of thermal treatment temperature on the leaching efficiency of Al from the samples pyrolyzed and incinerated between 400–700 °C for 30, 60, and 90 min are shown in Figure 1a,b. It can be seen that both thermal treatments show a maximum of 3.5% Al leaching efficiency at 700 °C. At higher temperatures, the concentration of Al was found to increase by nearly 50% in the sample treated at 700 °C, compared to the untreated sample, under both types of thermal treatment processes. Also, the Al leaching efficiency of the untreated sample was 0.47%. The low leaching efficiency of Al can be considered positive for the further obtainment of a lithium product, for example by evaporative crystallization, with higher purity.

3.8. Effect of L/S Ratio on the Leaching Efficiency of Al

The effect of L/S ratio on leaching of Al performed at 80 °C, stirring of 300 rpm for 3 h at two different L/S ratios of 10:1 and 20:1 mL g^{-1}, from samples pyrolyzed and incinerated between 400 and 700 °C for 30, 60, and 90 min is shown in the Figure 8a,b. It can be seen that leaching efficiency obtained at both the conditions at different L/S show similar trends, but the efficiency increases with increasing L/S ratio. A higher L/S ratio results in higher leaching efficiency when the dissolution of Al is limited by the solubility.

3.9. Effect of Leaching Temperature on the Leaching Efficiency of Al

The effect of leaching temperature on leaching of Al performed at stirring of 300 rpm for 3 h with an L/S ratio 20:1 mL g^{-1} at two different leaching temperatures: 80 °C and RT

from samples pyrolyzed and incinerated between 400 and 700 °C for 30, 60, and 90 min is shown in the Figure 9a,b. It is evident that the leaching of Al increases with an increase in the temperature. However, Al leaching efficiency of less than 0.5% and almost no leaching from pyrolyzed and incinerated samples, respectively, were observed at RT. This is because the solubility of the AlF_3 increases with an increase in the temperature. For example, the aqueous solubility of AlF_3 at 25 °C and 100 °C is 0.5 and 1.28 g/100 mL, respectively [18].

3.10. Effect of Addition of Excess Carbon

The effect of using excess carbon on leaching of Al performed at a stirring of 300 rpm for 1 h with an L/S ratio 20:1 mL g^{-1} at 80 °C from samples pyrolyzed at 400, 500, 600, and 700 °C for 30 min is shown in Figure 7. It can be observed that not much variation in leaching of Al was observed having additional carbon during the thermal treatment and the efficiency was less than 3%. Therefore, the addition of excess carbon did not have much effect on Al leaching.
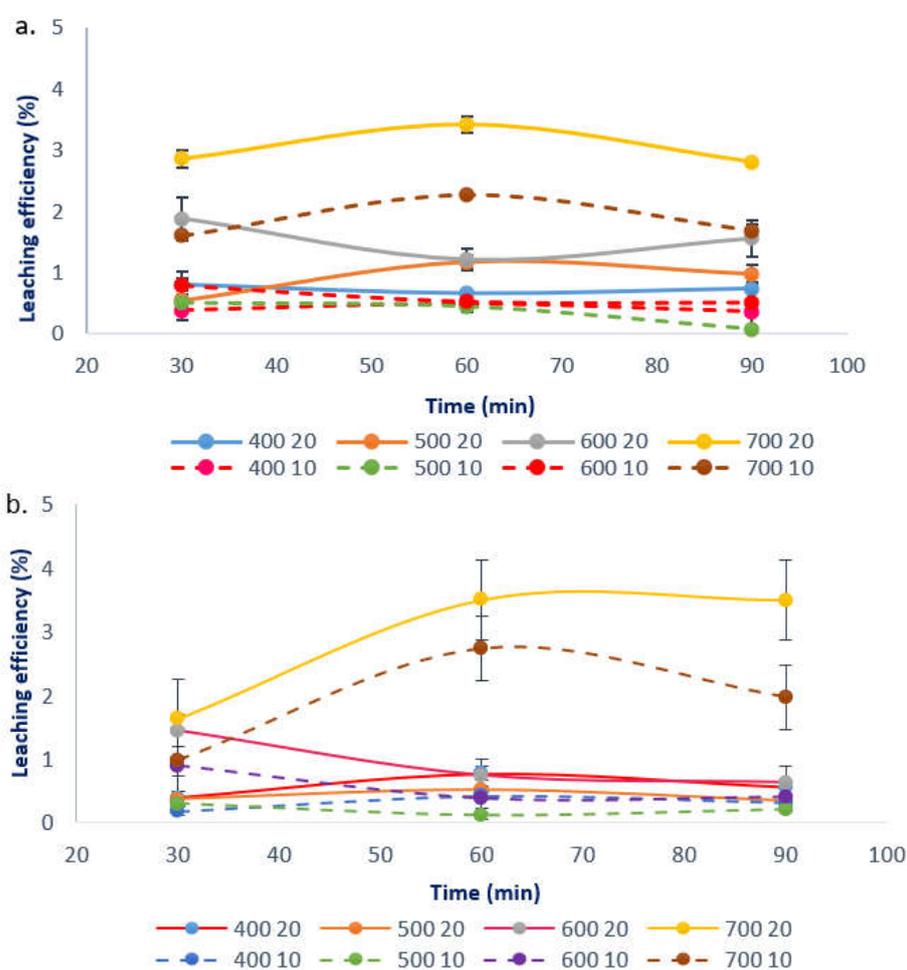

Figure 8. The effect of L/S ratio on Al leaching efficiency: (**a**) pyrolysis and (**b**) incineration (Leaching condition: L/S ratio = 20:1 and 10:1 mL g^{-1}, 80 °C, 300 rpm, and 3 h).
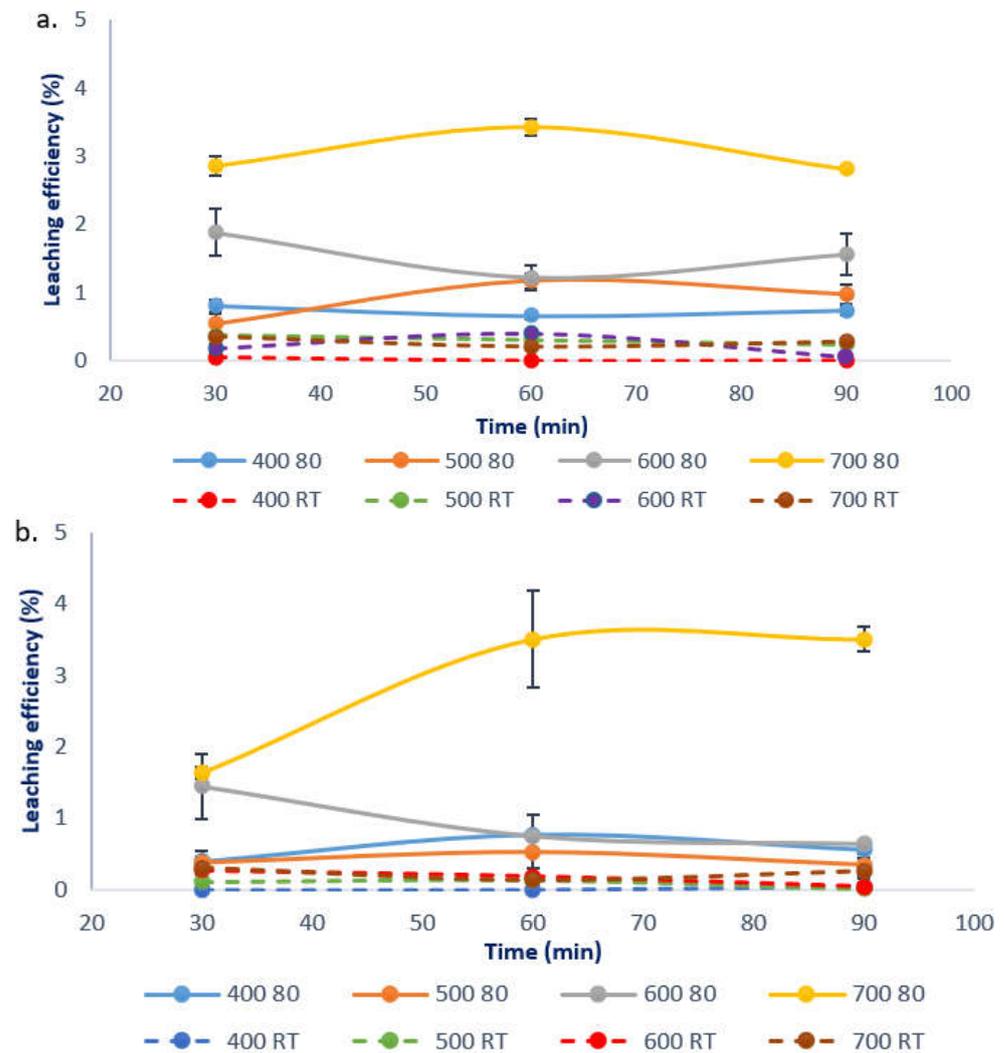
Figure 9. The effect of leaching temperature on Al leaching efficiency: (**a**) pyrolysis and (**b**) incineration (Leaching condition: (**a**). L/S ratio = 20:1 mL g^{-1}, 80 °C and RT, 300 rpm, and 3 h).

4. Conclusions

The leaching efficiency of Li from spent LIBs pretreated thermally by pyrolysis and incineration processes was investigated. The results show that Li could be separated and selectively recovered from the black mass. It was found that the leaching efficiency of Li from the pyrolyzed samples was higher than that from the incinerated samples. An increase in the thermal pretreatment temperature from 400 to 700 °C resulted in an increase in Li leaching efficiency, which could be favored by the removal of organic compounds such as the binder, which can hinder the recovery of Li from the electrode materials. Furthermore, the time of thermal pretreatment does not have much influence on the Li leaching efficiency, which might be due to the conversion of lithium metal oxides into Li salts within 30 min. After longer times, there might be an incomplete conversion of Li_2O to Li_2CO_3 due to the removal of gaseous products such as CO and CO_2 by the constant flow of N_2 needed for the reduction during pyrolysis. During the incineration, most of the carbon was lost after 30 min of treatment due to oxidation and much less remained for carbothermic reduction of metal oxides. However, the highest Li leaching efficiency of nearly 60% was observed from the sample pyrolyzed at 700 °C for 60 min and water leached under an L/S ratio of 20:1 mL g^{-1} at 80 °C and 300 rpm for 3 h. The results from the comparison of the effect of L/S ratio on leaching of Li performed at 80 °C, showed that the leaching efficiency of Li was higher with higher L/S ratio. At a higher leaching temperature, the leaching of Li is

higher due to an increase in the solubility of Li salts at higher temperatures. Additionally, the formation of LiF was observed by the reaction of Li_2O and Li_2CO_3 with HF generated by the decomposition of the PVDF binder. The reason for low Li efficiency (60%) could be due to unreacted NMC cathode materials during thermal treatment or incomplete leaching of Li salts and oxides by water. Therefore, to enhance the efficiency, tests were conducted using 10% of excess carbon in the form of graphite. However, there was no significant improvement in the leaching efficiency. The reason could be due to the stability of graphite which might not have completely taken part in the reduction process. Furthermore, some Al was also found to be leached with a leaching efficiency not higher than 3.5%.

Author Contributions: Conceptualization, methodology, software: S.B., N.V. and M.P.; validation: S.B., N.V., K.F. and M.P., formal analysis, investigation, data curation: S.B., T.L. and G.L. resources, M.P.; writing—original draft preparation: S.B.; writing—review and editing, visualization, supervision, M.P, N.V. and K.F.; project administration, M.P..; funding acquisition, M.P. All authors have read and agreed to the published version of the manuscript."

Institutional Review Board Statement: Not applicable.

Informed Consent Statement: Not applicable.

Data Availability Statement: The data presented in this study are available on request from the corresponding author.

Conflicts of Interest: The authors declare no conflict of interest.

References

1. Drabik, E.; Rizos, V. Prospects for electric vehicle batteries in a circular economy. *CEPS Res. Rep.* **2018**, 20.
2. Li, J.; Wang, G.; Xu, Z. Environmentally-friendly oxygen-free roasting/wet magnetic separation technology for in situ recycling cobalt, lithium carbonate and graphite from spent LiCoO2/graphite lithium batteries. *J. Hazard. Mater.* **2016**, *302*, 97–104. [CrossRef] [PubMed]
3. Söderman, M.L.; Kushnir, D.; Sandén, B. Will metal scarcity limit the use of electric vehicles? *Syst. Perspect. Electromobility* **2013**, 76–89.
4. Peng, C.; Liu, W.; Wang, Z.; Wilson, B.P.; Lundström, M. Selective extraction of lithium (Li) and preparation of battery grade lithium carbonate (Li_2CO_3) from spent Li-ion batteries in nitrate system. *J. Power Sources* **2019**, *415*, 179–188. [CrossRef]
5. Greim, P.; Solomon, A.A.; Breyer, C. Assessment of lithium criticality in the global energy transition and addressing policy gaps in transportation. *Nat. Commun.* **2020**, *11*, 4570. [CrossRef] [PubMed]
6. Agusdinata, D.B.; Liu, W.; Eakin, H.; Romero, H. Socio-environmental impacts of lithium mineral extraction: Towards a research agenda. *Environ. Res. Lett.* **2018**, *13*, 123001. [CrossRef]
7. Wanger, T.C. The Lithium future—Resources, recycling, and the environment. *Conserv. Lett.* **2011**, *4*, 202–206. [CrossRef]
8. European Commission. *Study on the EU's List of Critical Raw Materials—Final Report (2020)*; European Commission: Brussels, Belgium, 2020.
9. Graedel, T.E.; Allwood, J.; Birat, J.P.; Reck, B.K.; Sibley, S.F.; Sonnemann, G.; Buchert, M.; Hageluken, C. *Recycling Rates of Metals—A Status Report. A Report of the Working Group on the Global Metal Flow to the International Resource Panel*; UNEP: Nairobi, Kenya, 2011.
10. Zhao, Y.; Liu, B.; Zhang, L.; Guo, S. Microwave-absorbing properties of cathode material during reduction roasting for spent lithium-ion battery recycling. *J. Hazard. Mater.* **2020**, *384*, 121487. [CrossRef] [PubMed]
11. Xiao, J.; Li, J.; Xu, Z. Novel approach for in situ recovery of lithium carbonate from spent lithium ion batteries using vacuum metallurgy. *Environ. Sci. Technol.* **2017**, *51*, 11960–11966. [CrossRef] [PubMed]
12. Lombardo, G. Effects of Pyrolysis and Incineration on the Chemical Composition of Li-Ion Batteries and Analysis of the by-Products. Ph.D. Thesis, Chalmers University of Technology, Goteborg, Sweden, 2019.
13. Ekberg, C.; Petranikova, M. Lithium Batteries Recycling. In *Lithium Process Chemistry*; Elsevier Inc.: Amsterdam, The Netherlands, 2015; pp. 233–267. ISBN 978-0-12-801417-2.
14. Kuzuhara, S.; Ota, M.; Tsugita, F.; Kasuya, R. Recovering lithium from the cathode active material in lithium-ion batteries via thermal decomposition. *Metals* **2020**, *10*, 433. [CrossRef]
15. Liu, P.; Xiao, L.; Tang, Y.; Chen, Y.; Ye, L.; Zhu, Y. Study on the reduction roasting of spent $LiNi_xCo_yMn_zO_2$ lithium-ion battery cathode materials. *J. Therm. Anal. Calorim.* **2019**, *136*, 1323–1332. [CrossRef]
16. Jandova, J.; Dvorak, P.; Kondas, J.; Havlak, L. Recovery of lithium from waste materials. *Ceram. Silikáty* **2012**, *56*, 50–54.

17. Paulino, J.F.; Busnardo, N.G.; Afonso, J.C. Recovery of valuable elements from spent Li-batteries. *J. Hazard. Mater.* **2008**, *150*, 843–849. [CrossRef] [PubMed]
18. Lide, D.R. *CRC Handbook of Chemistry and Physics*; Internet Version 2005; CRC Press: Boca Raton, FL, USA, 2005. Available online: http://www.hbcpnetbase.com (accessed on 12 December 2020).
19. Xue, S.; Zhang, L.; Han, Z.; Huang, X. Reaction mechanism between oxide film on surface of Al-Li alloy and CsF-AlF_3 flux. *Trans. Nonferrrous Met. Soc. China* **2008**, *18*, 121–125. [CrossRef]
20. Schwich, L.; Schubert, T.; Friedrich, B. Early-Stage Recovery of Lithium from Tailored Thermal Conditioned Black Mass Part I: Mobilizing Lithium via Supercritical CO_2-Carbonation. *Metals* **2021**, *11*, 177. [CrossRef]
21. Zheng, J.M.; Zhang, Z.R.; Xu, X.B.; Dong, Z.X.; Zhu, Z.; Yang, Y. The effect of AlF_3 coating on the performance of Li[Li0.2Mn0.54Ni0.13Co0.13]O_2 positive electrode material for lithium-ion battery. *J. Electrochem. Soc.* **2008**, *155*, A775–A782. [CrossRef]
22. Julien, C.M.; Mauger, A. Functional behavior of AlF3 coatings for high-performance cathode materials for lithium-ion batteries. *AIMS Mater. Sci.* **2019**, *6*, 406–440. [CrossRef]
23. Vargel, C. Inorganic Acids. In *Corrosion of Aluminium*; Elsevier: Amsterdam, The Netherlands, 2004; pp. 397–414, ISBN 9780080444956. [CrossRef]
24. Cano, A.M.; Marquardt, A.E.; DuMont, J.M.; George, S.M. Effect of HF pressure on Thermal Al_2O_3 atomic layer etch rates and Al_2O_3 fluorination. *J. Phys. Chem.* **2019**, *123*, 10346–10355. [CrossRef]